

Project Number 282910

ÉCLAIRE

**Effects of Climate Change on Air Pollution Impacts and Response
 Strategies for European Ecosystems**

Seventh Framework Programme

Theme: Environment

**D4.4. A vertically-resolved, multi-layer in-canopy chemical processing
 model of NO-NO₂-O₃-VOCs and NH₃-HNO₃-NH₄NO₃ exchange**

Due date of deliverable: **31/03/2014**

Actual submission date: **30/09/2015**

Start Date of Project: **01/10/2011**

Duration: **48 months**

Organisation name of lead contractor for this deliverable :
INSTITUT NATIONAL DE LA RECHERCHE AGRONOMIQUE

Project co-funded by the European Commission within the Seventh Framework Programme		
Dissemination Level		
PU	Public	<input checked="" type="checkbox"/>
PP	Restricted to other programme participants (including the Commission Services)	<input type="checkbox"/>
RE	Restricted to a group specified by the consortium (including the Commission Services)	<input type="checkbox"/>
CO	Confidential, only for members of the consortium (including the Commission Services)	<input type="checkbox"/>

1. Executive Summary

For accomplishing this Deliverable, a new multi-layer surface exchange model (ÉCLAIRE Surface Exchange model, ESX) was developed and tested against flux data collected within ÉCLAIRE. In addition, the Multi-Layer Canopy Chemical Exchange Model (MLC-CHEM) system was extended and applied in an analysis of atmosphere–biosphere interactions and feedbacks.

ESX was formulated as a generic mathematical framework, based on the one-dimensional, time-dependent conservation equation for atmospheric mixing ratios that are controlled by turbulent mixing, atmospheric chemistry and surface exchange. The formulation includes an option for a description of bi-directional exchange with the mesophyll, external leaf surfaces, non-leaf surfaces and soil. The modelling of vertical mixing relies on the first order turbulence closure. A variety of chemical schemes are available for ESX from the EMEP chemistry transport model (CTM) system. ESX can already be run in a stand-alone mode, providing a tool for site-specific process analysis, and it will be included as an advanced deposition/emission module in the EMEP CTM. For minimizing the computational cost when implemented in a CTM, a new subgrid algorithm was developed for ESX.

ESX resolves the vertical distribution of the key variables that characterize atmosphere–vegetation interactions, i.e. concentration, source/sink exchange rate, source/sink flux density per leaf area, separating the emission and deposition fluxes, and turbulent mixing and chemical reaction rates. This makes it a useful tool for analysing field measurements and developing advanced risk assessment methods for pollution impacts, for example. Simulations with ESX demonstrated the complex interplay between biogenic emissions, turbulent mixing, chemical reactions, deposition and advection within and above the vegetation layer.

ESX was tested against the data from ÉCLAIRE measurements at Hyytiälä, Finland. A comparison of measured deposition velocities with those calculated with different configurations of ESX showed that inclusion of an explicit description of the forest understory, in addition to the Scots pine canopy, improves the performance of ESX. A further improvement was obtained by enhancing the stomatal limitation due to water vapour pressure deficit.

In addition to the development of a new surface exchange model, the work for this Deliverable involved further development of MLC-CHEM. This model, which constitutes a component of a global chemistry–climate modelling system that can also be run as a 1-D model, was extended and can now be used as a multi-layer stand-alone version for site-specific studies. Furthermore, a coupling to the dynamic global vegetation model LPJ-GUESS was developed for studying interaction between surface exchange and climate.

The site-specific simulations with MLC-CHEM demonstrated the potential of multi-layer models, such as MLC-CHEM and ESX, for enhancing the interpretation of measurement data and for supporting the design of new field campaigns. The observed NO_x concentrations in a deciduous forest were compared with those modelled with MLC-CHEM with different assumptions on leaf-scale NO_x exchange. This comparison indicated that the best agreement can be achieved by introducing a leaf-scale compensation point for NO₂. These results provided guidance for pursuing follow-up measurements to better understand the role of the compensation points in NO_x exchange.

The coupled MLC-CHEM/LPJ-GUESS system was applied in a study of the interactions between ozone deposition to vegetation, impacts on primary production and biogenic emissions producing ozone in the atmospheric boundary layer. A ~100-yr offline LPJ-GUESS simulation of ecosystem dynamics, followed by a fully coupled seasonal MLC-CHEM/LPJ-GUESS simulation, suggested that the detrimental impact of ozone on net primary productivity reduces evapotranspiration rates. Thus changes in the hydrological cycle potentially play a significant role in feedback processes involved in the atmosphere–biosphere interactions.

Objectives:

- Evaluation and improvement of a computationally efficient coupled multi-layer exchange and chemistry model for site- to global-scale simulations of in-canopy interactions and net exchange fluxes
- Extension of an existing scheme for the NO-NO₂-O₃-VOCs system and the dependence on in-canopy turbulence, to treat the phase partitioning of the NH₃-HNO₃-NH₄NO₃ system
- Assessment and fine-tuning of the model framework against data from the ÉCLAIRE intensive campaigns (WP1) and other suitable datasets and compared against the single-layer approaches
- multi-layer model investigations of the vertical distribution of O₃ concentration and sinks within the canopy, resulting from gradients in irradiance, stomatal conductance and surface wetness

2. Activities:

- mathematical formulation of a new multi-layer model (ÉCLAIRE Surface Exchange model, ESX)
- development and testing of the Fortran code for ESX
- testing and validation of ESX against field measurements
- further development Multi-Layer Chemical Exchange Model (MLC-CHEM) and coupling with the dynamic global vegetation model LPJ-GUESS
- application of the coupled MLC-CHEM/LPJ-GUESS system to feedbacks involved in ozone deposition

3. Results:

- a new multi-layer model (ESX), suitable for incorporation into chemical transport models (CTMs), has been developed (Annex 1)
- a new sub-grid algorithm has been developed, making it possible to minimize the number of model layers when ESX is incorporated into a CTM (Annex 1)
- detailed vertical profiles of concentrations and different stomatal and non-stomatal flux components, separating emission and deposition, can be simulated, e.g. for ozone risk assessment (Annex 1)
- mixing ratios of reactive compounds show complex and temporally varying vertical profiles within and above the vegetation layer, resulting from the interplay between biogenic emissions, chemistry, turbulent mixing and deposition (Annex 1)
- model performance for ozone deposition to a coniferous forest can be improved by introducing an explicit understory layer in the model (Annex 1)
- an improved stand-alone version and coupling to LPJ-GUESS have been developed for the MLC-CHEM system (Annex 2)
- coupled MLC-CHEM/LPJ-GUESS simulations reveal potentially significant interactions between pollution impacts on vegetation, boundary-layer dynamics and the hydrological cycle (Annex 2)
- inclusion of a leaf-scale compensation point for NO₂ improves the agreement of MLM-CHEM simulations with measurement data from a deciduous forest (Annex 2)

4. Milestones achieved:

- MS18: Incorporation of results from flux monitoring data generated within ÉCLAIRE into modelling framework

ÉCLAIRE data from the Hyytiälä flux site have been extensively used in the development of the ESX model. Configuration of ESX for the data collected within the ÉCLAIRE intensive campaign at Bosco Fontana is in progress.

5. Deviations and reasons:

Delivery of D4.4 was delayed until the final month of ÉCLAIRE, because the major part of the activities for accomplishing this Deliverable was focused on developing a new multi-layer surface exchange model (ESX) rather than re-parameterising existing models.

6. Publications:

- Cieslik, S., Tuovinen, J.-P., Baumgarten, M., Matyssek, R., Brito, P. and Wieser, G., 2013. Gaseous exchange between forests and the atmosphere. *Developments in Environmental Science* 13, 19–36.
- Simpson, D. and Tuovinen, J.-P., 2014. ECLAIRE Ecosystem Surface Exchange model (ESX). In: *Transboundary particulate matter, photo-oxidants, acidifying and eutrophying components. EMEP Status Report 1/2014*, Norwegian Meteorological Institute, pp. 147–154.

7. Meetings:

In addition to the annual ÉCLAIRE General Assemblies:

- ÉCLAIRE meeting on resistance model harmonisation, Edinburgh, 19–21 March 2012
- ESX work meeting, Bonn, 7–8 May 2013
- ESX–DEWS work meeting, Amsterdam, 29 August 2013
- C1–ESX work meeting, Edinburgh, 26–28 May 2014
- ESX–DEWS work meeting, Gothenburg, 26–29 August 2014

8. List of Documents/Annexes:

Annex 1: Development of a new multi-layer surface exchange model (ESX)

Annex 2: Simulations with the improved MLM-CHEM system

Annex 1: Development of a new multi-layer surface exchange model (ESX)

1 Introduction

Numerical models that simulate both chemistry and transport of gases and aerosols are essential tools for understanding the atmosphere, and for developing policy measures designed to tackle air pollution and other environmental problems. Three-dimensional chemistry transport models (CTMs) are used to estimate concentrations of pollutants such as ozone and to map acidifying and eutrophying deposition across large areas; examples of such CTMs include the EMEP MSC-W model (Simpson et al., 2012), CMAQ, (Foley et al., 2010) and the models used in IPCC assessments (Lamarque et al., 2013). These models operate with horizontal grid sizes of at best several km and at worst several degrees of longitude/latitude. They are well suited to simulating the large-scale advection and chemical processing of air masses, but they are necessarily highly simplified with regard to the exchange of pollutants between the atmosphere and biosphere. For example, most models regard vegetated surfaces, even tall forests, as thin, flat surfaces – the so-called ‘big-leaf’ approach. Mass exchange, i.e. deposition and emission, at these hypothetical surfaces is derived from the large volumes associated with the bottom layers of the CTMs.

The simplification of the atmosphere–ecosystem interactions is a concern, since the processes governing the exchange are known to be complex, with small-scale turbulence and non-linear chemical processing causing sometimes major deviations from the results expected from simple big-leaf approaches (Fowler et al., 2009). For example, forests constitute major deposition sinks for ozone (Cieslik et al., 2013), nitrogen compounds (Eugster and Haeni, 2013) and indeed most reactive gases and particles (Fowler et al., 2009). However, forests are also a major source of biogenic volatile organic compounds (BVOCs), which are important precursors to ozone and secondary organic aerosols (Guenther et al., 1995; Simpson, 1995; Bergström et al., 2012; Carslaw et al., 2013). Chemical reaction time-scales in forest canopies can be very short (minutes), so that some emitted species sometimes do not even leave the canopy, but are transformed to other gases or aerosols (Kramm et al., 1995; Ganzeveld et al., 2008). These interactions within and just above the trees are typically completely ignored by the large-scale CTMs.

Another major challenge for large-scale CTMs is the incorporation of interactions between emissions of gaseous NH_3 and HNO_3 and ammonium nitrate aerosol. Indeed, NH_3 may be emitted from or deposited to ecosystems, depending upon the level of NH_4^+ in the soil and the apoplast of vegetation (Sutton et al., 1995; Nemitz et al., 2004; Flechard et al., 2013). Although there have been some attempts to cope with such bi-directional exchanges in modified big-leaf approaches in CTMs (Zhang et al., 2010; Wichink Kruit et al., 2012; Pleim et al., 2013), the heterogeneities of sources/sinks, temperature, humidity and

dispersion conditions lead to complex vertical concentration gradients and chemical flux divergence, which complicate both modelling and measurement analysis (Nemitz et al., 2004; Fowler et al., 2009).

Within Europe, the European Monitoring and Evaluation Programme (EMEP, www.emep.int) is responsible for estimating the fields of pollutant concentrations and depositions, including transboundary pollution fluxes. The EMEP MSC-W model (Simpson et al., 2012), developed for this purpose, is a 3-D Eulerian CTM which is typically run with horizontal grid-sizes of around 20–50 km for European simulations, although it has also been adopted to both fine-scale, e.g. 5–7 km resolution (Vieno et al., 2010; Schaap et al., 2015), and global-scale (Jonson et al., 2010) modelling. The height of the bottom layer of the EMEP MSC-W model is ca. 90 m.

One of the major tasks for the EMEP MSC-W model is to make predictions of pollutant fluxes to vegetation, for estimating atmospheric nitrogen supply and potentially deleterious ozone uptake, for example, both for current conditions and future scenarios (Simpson et al., 2007; Fagerli and Aas, 2008; Tuovinen et al., 2009; Simpson et al., 2014). The accuracy of such predictions largely depends on the description of biosphere–atmosphere exchange processes. However, the modelling (and indeed understanding) of such exchanges is fraught with difficulties because of the near-surface complexities highlighted above.

A large number of 1-D CTMs have been built, offering some solution to the above problems. As examples of earlier efforts, we refer to Hov (1983), who modelled the short-term dynamics of about 40 chemical species in the atmospheric boundary layer, including a highly simplified treatment of dry deposition; to Meyers and Baldocchi (1988), who tested multi-layer canopy deposition models with no chemistry; and to Gao et al. (1993), who incorporated a multi-layer surface exchange model into a coupled diffusion–chemistry model to study the vertical concentration and flux profiles of reactive trace gases. A summary of more recent 1-D models can be found in Saylor (2013). By allowing the 1-D column to move along air mass trajectories, a Lagrangian implementation of such models can also be achieved (e.g. Hertel et al., 1995). However, many of these models are no longer operational, and those that are are generally not released in the public domain. In any case, such models often deal with a limited part of the problem; e.g. they focus on forests but not grasslands, or on ozone chemistry but not nitrogen exchange. Such 1-D models also tend to be constructed for research purposes, with computational efficiency not being a priority, and often provide little flexibility in terms of the number of layers or chemical schemes.

In order to bridge the gap between the needs of scientifically complex canopy models and large-scale 3-D CTMs, a new 1-D surface exchange model, called ESX, has been developed within ÉCLAIRE. The structure of the ESX code specifically aims at an integration into the modelling system of EMEP MSC-W, in which it will serve as an advanced dry deposition module that will replace the present big-leaf-based parameterisation. For site-specific analysis, ESX can already be run in a stand-alone mode, with input data and boundary conditions either being set in configuration files or obtained from the EMEP CTM

data or directly from in-situ measurements. The ESX code is written in Fortran 90/95 (with traces of F2003/2008). A summary of the model formulation and some test results are presented below.

2 Model description

2.1 Basic structure

The basic formulation chosen for ESX is the one-dimensional conservation equation

$$\rho \frac{\partial \xi}{\partial t} = - \frac{\partial \varphi}{\partial z} + S$$

where ξ is scalar mixing ratio, ρ is air density, φ is vertical flux density, and S represents sources and sinks. The latter includes, in addition to chemical kinetics, generic first (D) and zeroth (E) order deposition and emission terms

$$S_{\text{ex}}(z) = D(z)\chi(z) + E(z) \quad (2)$$

Within ESX these terms are formulated so as to account for bi-directional exchange occurring at the surfaces of vegetation. Similarly, the lower boundary condition of Eq. (1) provides a flexible interface for including soil emission and deposition fluxes in different ways:

$$\varphi(0) = F_1\chi(0) + F_0$$

where $\chi = \rho\xi$ is scalar density, and F_1 and F_0 the first and zeroth order coefficients, respectively. A corresponding condition is set for the upper boundary, the specific form of which depending on the application; for example, a fixed concentration can be set.

The deposition/emission fluxes are formulated using the common approach of electrical analogy. Figure 1 depicts the exchange pathways in terms of this analogy. There are three potential exchange targets within the vegetation canopy: the mesophyll, external leaf surfaces and non-leaf vegetation surfaces. The ESX structure allows for bi-directional exchange for all of these, and similarly for the soil exchange, by defining a ‘compensation point’ or a non-zero boundary condition concentration at each interface, typically estimated from equilibrium considerations with the apoplast or soil medium.

The leaf exchange, both stomatal and non-stomatal, is defined separately for the adaxial and abaxial leaf surfaces ($j = 1, 2$). The canopy exchange can be expressed by writing the corresponding source/sink term, Eq. (2), as

$$S_{\text{ex}} = \sum_{j=1}^2 [g_{\text{sm},j}(\chi_{\text{s},j} - \chi_{\text{c},j}) + g_{\text{ns},j}(\chi_{\text{ns},j} - \chi_{\text{c},j})] a_{\ell} + g_{\text{nl},j}(\chi_{\text{nl},j} - \chi_{\text{c},\text{nl}}) a_{\text{nl}}$$

where $g_{\text{sm},j}$ combines stomatal conductance $g_{\text{s},j}$ and mesophyll conductance $g_{\text{m},j}$, and other notation is explained in Figure 1. All terms in Eq. (4) are height- and time-dependent. The leaf-level exchange, Eq.

(4), is coupled with atmospheric mixing, Eq. (1), via the boundary layers that encompass the vegetation surfaces and are modelled with the g_b terms in Figure 1. Based on this coupling, we can derive expressions for the D and E terms in Eq. (2):

$$D = - \sum_{j=1}^2 \frac{g_{b,j}(g_{sm,j} + g_{ns,j})}{g_{sum,j}} a_\ell - \frac{g_{b,n\ell} g_{n\ell}}{g_{b,n\ell} + g_{n\ell}} a_{n\ell}$$

$$E = \sum_{j=1}^2 \left(\frac{g_{b,j} g_{sm,j}}{g_{sum,j}} \chi_{s,j} + \frac{g_{b,j} g_{ns,j}}{g_{sum,j}} \chi_{ns,j} \right) a_\ell + \frac{g_{b,n\ell} g_{n\ell}}{g_{b,n\ell} + g_{n\ell}} \chi_{n\ell} a_{n\ell}$$

where $g_{sum,j} = g_{b,j} + g_{sm,j} + g_{ns,j}$. Bi-directional exchange at the soil-atmosphere is realized with a series of standard big-leaf resistances that are connected to soil compensation point (χ_g in Fig. 1).

2.2 Turbulent mixing

Modelling of vertical mixing is based on the first order turbulence closure

$$\varphi = -\rho K_z \frac{\partial \xi}{\partial z}$$

where K_z is eddy diffusivity (Fig. 1). As a default, the K_z profile within and just above the canopy is calculated in ESX using the approach of Leuning (2000) with a minor modification introduced to ensure the continuity of the K_z profile. In this approach, eddy diffusivity is expressed as

$$K_z(z) = \frac{\tau_L \sigma_w^2}{\phi_h(\zeta)}$$

where τ_L is the Lagrangian time scale of turbulence, σ_w is the standard deviation of vertical wind velocity and the function ϕ_h accounts for the influence of atmospheric stability. The vertical profiles of τ_L and σ_w depend on vegetation height and friction velocity. Optionally, a correction factor developed by Makar et al. (1999) can be added as a multiplier of the K_z derived from Eq. (7).

Including the stability correction in Eq. (7) means that we assume the Monin–Obukhov similarity theory of the inertial sublayer to be valid also within the roughness sublayer. At the top of the surface layer, this profile is matched to the K_z used within the EMEP MSC-W model (Simpson et al., 2012). Examples of in-canopy residence times calculated with ESX are presented in ÉCLAIRE Deliverable 7.3.

2.3 Chemistry

As with the standard EMEP CTM, a variety of chemical schemes are available for ESX (Table 1). New schemes can be readily added by a chemical pre-processor (GenChem), which is part of the EMEP modelling system (Simpson et al., 2012). GenChem generates the Fortran code needed for solving the differential equations representing chemical reactions.

Table 1. Chemical schemes operational in ESX.

Mechanism	No of species	No of reactions	No of BVOCs	Comments
ESX-F19	19	11	0	Minimal scheme, for testing
EmChem09	72	137	1	EMEP standard ^a (Simpson et al., 2012)
EmChem09-ESX	72+5	137+16	1+3	ESX standard ^b
CB05	70	189	2	Carbon bond (Yarwood et al., 2005)
CRI v2	465	1202	3	Condensed version of Master Chemical Mechanism (Jenkin et al., 2008)
CRI v2 R5	195	569	2	(Archibald et al., 2010)

^aNumbers refer to the default EMEP chemistry where only isoprene is included for BVOCs. Some tracer species are excluded. An α -pinene chemistry is available for organic aerosol studies.

^bAdds some monoterpene and sesquiterpene species and reactions to EmChem09.

The standard ‘EmChem09’ scheme derived from the EMEP MSC-W model has only isoprene chemistry, although expanded versions are available when tackling secondary organic aerosol formation from monoterpenes (Bergström et al., 2012). Considering the more comprehensive chemical schemes in the EMEP/ESX system, the ‘CRI v5’ scheme has isoprene, α -pinene and β -pinene mechanisms, and ‘CRI v2’ has in addition 3-methyl-2-buten-2-ol (MBO).

For the ESX work, we have extended the basic ‘EmChem09’ scheme with two surrogate monoterpene species: α -pinene (70% of monoterpene emissions) and limonene (30%). We assume further a sesquiterpene (surrogate β -caryophyllene) emission rate of 10% of monoterpene emissions (see ÉCLAIRE Deliverable 7.3). For α -pinene we use the simple mechanism of Makar et al. (1999). For limonene and β -caryophyllene we use simplified mechanisms based on Wolfe and Thornton (2011).

2.4 Numerical methods

Chemical kinetics are separated from the overall problem of Eq. (1) with an operator splitting technique and solved with the TWOSTEP method implemented in the EMEP CTM (Verwer and Simpson, 1995). The remaining problem encompassing vertical mixing and surface exchange processes is solved with a mass-conserving finite volume method and semi-implicit Crank-Nicolson time differencing (e.g.

Patankar, 1980). In principle, ESX makes it possible to define any number of computation layers of arbitrary depth within and above the vegetation.

The numerical finite volume method and its implementation have been verified with analytical solutions available for simplified cases (power-law K_z profile with no sources/sinks; constant K_z profile with ground removal). An example of the good agreement between numerical and analytical solutions is shown in Figure 2. The mixing algorithm has also been shown to produce results very similar to those obtained from a stochastic Lagrangian particle model. The mass balance is verified within the ESX code at each time step.

In ESX, S_{ex} and K_z , Eqs. (4) and (7), are calculated as 'effective' values that incorporate sub-grid information within the model layer. For the source/sink term this means that all the conductance and other terms contributing to S_{ex} are first evaluated at several (five) points within each layer and the grid-point value used in solving Eq. (1) is obtained by numerical integration with the Legendre-Gauss quadrature. The definition of effective K_z is presented in Figure 3. This novel feature makes it possible to minimize the number of the actual model layers that are needed to adequately resolve the vertical gradients especially within and just above vegetation, thus reducing the overall computational cost.

2.5 Parameterisations

Vegetation is described by area distributions of leaves and other external plant surfaces (a_ℓ and $a_{n\ell}$ in Fig. 1), and there is an option for parallel vegetation distributions, allowing simultaneous inclusion of both trees and shrubs, for example.

ESX has two options for calculating stomatal conductance: (1) multiplicative response model and (2) photosynthesis-based model. The former option is implemented based on the EMEP/DO₃SE deposition algorithms included in the EMEP CTM (Simpson et al., 2012), while the latter makes use of the new DO₃SE parameterisations developed within ÉCLAIRE, including the DO₃SE-ESX interface coded for ESX (described within ÉCLAIRE Deliverable 4.3).

Within the multiplicative algorithm, the stomatal conductance is assumed to depend on irradiance, so the conductances within the sunlit and shaded leaf areas differ in magnitude. This is taken into account in the calculation of $g_{\text{sm},j}$ by areal weighting. The fraction of sunlit leaf area is assumed to decrease exponentially downwards from the canopy top as a function of accumulated vegetation surface area, $A_c(z)$. The vertical in-canopy distribution of photosynthetically active radiation is calculated according to the multi-layer adaptation of the Norman scheme by Zhang et al. (2001).

The non-stomatal conductance terms have so far been derived from the existing big-leaf parameterisations of the EMEP/DO₃SE deposition module. The new algorithms developed within ÉCLAIRE will be incorporated in the future, as far as is possible considering input data requirements.

The leaf-scale boundary layer conductance is calculated according to the aerodynamic flat-plate theory, and both forced and free convection conditions are allowed for. Leaf temperature is estimated by applying an energy balance model. The vertical profile of wind speed, which drives forced convection, is calculated from the canopy-top wind speed by assuming exponential attenuation as a function of A_c , as per Wolfe and Thornton (2011). The canopy-top wind speed is calculated from a reference value defined above the canopy by extrapolating the Monin–Obukhov wind profile used in the EMEP CTM.

3 Results

3.1 Examples of modelled profiles

ESX makes it possible to resolve the vertical distribution of the key variables that characterize atmosphere–vegetation interactions, i.e. concentration (mol m^{-3}), source/sink exchange rate ($\text{mol m}^{-3} \text{s}^{-1}$), source/sink flux density per leaf area ($\text{mol m}^{-2} \text{s}^{-1} \text{PLA}$) separating the emission and deposition fluxes, and turbulent mixing and chemical reaction rates ($\text{mol m}^{-3} \text{s}^{-1}$). Examples of modelled ozone concentration and flux profiles within and above a Scots pine forest are shown in Figure 4.

In the case of ozone, both the forest canopy and forest soil act as sink surfaces, the former being strongly variable due to environmental control of stomatal exchange. The simulations show that, while the overall concentration profile is expectedly affected by deposition, the canopy-induced local gradients are modest. In contrast, there is large flux divergence within the canopy layer, and (close-to-)constant-flux layers are formed both above the canopy and within the trunk space.

Figure 5 (top row) illustrates how the rate of stomatal sink evolves during the first half of a day, being zero during the night and then increasing with the increasing availability of photosynthetically active radiation. As extinction of the radiation available across the canopy is accounted for in ESX, the stomatal sink rate is not proportional to leaf area. Nearly proportional relationship is established for the non-stomatal sink rate (Fig. 5, 2nd row from top), which in these simulations is derived from a constant conductance term $g_{n\ell}$, with only a small perturbation from the wind speed profile to the boundary-layer conductance $g_{b,n\ell}$ and hence the ozone flux.

Risk assessment of detrimental ozone effects on vegetation is typically based on ambient concentration and, nowadays more commonly, on stomatal uptake (CLRTAP, 2014). This uptake is expressed as the stomatal flux density per leaf area, and risk indices have been developed which cut out a certain threshold flux to compensate for the detoxification capacity of plants. So far, these flux-based indices, most notably the Phytotoxic Ozone Dose above a threshold of Y (PODY) used within UNECE (CLRTAP, 2014), and the related dose-response relationships have only been derived for the sunlit leaves at the canopy top. Figure 5 (2nd row from bottom) shows that very large vertical flux gradients are to be

expected, which are further enhanced when introducing a threshold flux (Fig. 5, bottom row). These results demonstrate how a multi-layer model such as ESX could serve as a significantly improved tool, as compared to traditional one-layer models, enabling development of more realistic risk metrics.

The role of chemistry is discussed in more detail in ÉCLAIRE Deliverable D7.3, which is focused on the effect of NO emissions from soil and in-canopy emissions of VOCs on different deposition terms. However, we present here examples of ESX calculations that demonstrate the importance of modelling the vertical profiles of reactive compounds. Figure 6 shows the variations in NO, HNO₃, limonene (a BVOC) and NO₃ radical concentrations for a 12-h period over a forest with high emissions of BVOCs from the foliage and NO from the soil. In these calculations, concentrations of O₃ and other long-lived compounds from the EMEP CTM were used as 'advected' boundary conditions above 45 m. These concentrations are then modified within ESX by the BVOC and NO emissions as well as the other chemical and exchange processes modelled within the vertical column.

These calculations show, for example, a strong effect of the (admittedly high) soil-NO emissions on the near-ground NO concentrations – much higher values than seen above (Fig. 6). HNO₃, on the other hand, is also changing at higher levels due to changes in the advected concentrations. Within the canopy a mixture of processes operate in tandem, with HNO₃ deposition losses to the canopy and increases near the ground due to conversion of the soil-emitted NO through NO₂ chemistry.

The concentrations of limonene vary rather straightforwardly, with concentrations dropping to near zero at heights above 100 m (Fig. 6). This steep gradient is clearly reflected in the NO₃ profile: where limonene and other BVOCs are present, the night-time NO₃ concentration drops to zero due to rapid reaction with these compounds. Above the 'BVOC layer', the nocturnal NO₃ concentrations rise rapidly to high values. (The very high concentrations shown here are rather untypical, but reflect our high biogenic emission test configuration.) In daytime, NO₃ concentrations are minuscule simply due to its rapid photolysis.

3.2 Optimisation of the number of model layers

ESX has been developed to serve two purposes: (1) to act as a stand-alone tool for site-specific simulations, supporting data analysis and providing climate-change scenarios, for example, and (2) to act as a generic deposition module within a regional-scale CTM, in particular the EMEP MSC-W model. While in principle an arbitrarily large number of vertical layers can be used in the former application, ensuring sufficient vertical resolution, for the latter objective the number of layers needs to be minimized for computational cost.

Figure 7 shows results from a set of ESX calculations where the exchange parametrisations, meteorological conditions and vegetation distribution are identical in each run but vegetation height, h_v , and model layer depth, Δz , are varied. The error due to compromised resolution is calculated

for both the across-canopy integrated stomatal conductance and sink rate by taking the results for $\Delta z = 0.5$ m as reference. These errors show that even in a rather extreme case of $\Delta z = h_v$, i.e. when all vegetation (here forest canopy) is incorporated into a single model layer, the error remains limited, being consistently less than 10% for stomatal conductance. For the stomatal sink rate, the corresponding error is even smaller, less than 5% for any h_v , due to dynamical compensation effects.

The conclusions drawn from Figure 7 can be generalised for a longer simulation period. Figure 8 presents three-day time series for the downward flux/concentration ratio ('deposition velocity') above a forest canopy. For $h_v = 5$ m, for example, a layer resolution of $\Delta z = 5$ m produces results that are very similar to those calculated with $\Delta z = 1$ m. Similarly in the case of $h_v = 15$ m, throughout the diurnal cycle there are only relatively small differences between the deposition velocities calculated with $\Delta z = 1$ m and 15 m. Overall, these results indicate that the new sub-grid integration developed here for ESX makes it possible to implement a detailed multi-layer model in a CTM in a cost-effective manner.

3.3 Comparison against measurement data

The ESX model will be tested against data collected at different ÉCLAIRE measurement sites. The first tests have been carried out for Hyytiälä, Finland. This site is dominated by a 15-m-high Scots pine forest with a projected leaf area index of 2.5. On the forest floor there is a low shrub layer mainly consisting of lingonberry, bilberry and mosses.

In these tests, the downward flux/concentration ratio ('deposition velocity') of ozone calculated with ESX was compared against the values derived from ozone flux and concentration measurements at Hyytiälä in July 2011, which data were made available by the University of Helsinki. The meteorological input and chemical boundary conditions were obtained from the EMEP MSC-W modelling system. ESX was run over the one-month period by changing input on an hourly basis assuming that a steady state is established at the end of each hour. The upper boundary of the modelling domain was set at 45 m, which is the height of the lowest grid point of the EMEP CTM, and the concentrations at this height were fixed to those provided by that model.

First, ESX was run with exchange parameters derived from the existing dry deposition module of the EMEP model (Simpson et al., 2012). In this ESX version (below referred to as 'Default'), deposition to ground surface is controlled by big-leaf resistances R_{bg} and R_g (Fig. 1), with R_g set to a constant value. For a second set of ESX runs ('Shrub' version), this was replaced by an explicit description of the forest understory layer, where vertical mixing and stomatal and non-stomatal exchange were modelled the same way as for the tree canopy. This change resulted in a significant improvement in the model performance, this version outdoing the standard big-leaf EMEP/DO₃SE model (Table 2, Fig. 9). The overestimation by the model was significantly reduced, and the correlation between the hourly values was increased when introducing an additional vegetation distribution.

Table 2. Mean measured and modelled deposition velocity of ozone and related performance statistics of the big-leaf EMEP/DO₃SE and multi-layer ESX models at Hyytiälä, Finland in July 2011.

	Measured	Modelled			
		Big-leaf	Default	Shrub	Shrub + VPD
Mean (cm s ⁻¹)					
day ^a	0.491	0.636	0.706	0.550	0.508
night ^b	0.192	0.202	0.261	0.172	0.171
RMSE ^c (cm s ⁻¹)		0.231	0.263	0.199	0.195
NMB ^d		24.5%	41.4%	7.1%	0.1%
Correlation		0.660	0.669	0.689	0.694

^a5:30 a.m. – 8:30 p.m.; ^b8:30 p.m. – 5:30 a.m. ^cRoot Mean Square Error; ^dNormalized Mean Bias

Despite the overall improvement of model performance (Table 2) and an accurate prediction of the nocturnal minimum (Fig. 9), the ‘Shrub’ configuration of ESX did not fully replicate the shape of the observed mean diurnal cycle, on average showing too large deposition velocities during the late afternoon hours. As a potential explanation for this discrepancy, an additional test was performed by changing the response of stomatal conductance to air humidity by enhancing the limiting effect of water vapour pressure deficit (VPD) (‘Shrub + VPD’ version). While this modification effectively eliminated any remaining bias and slightly improved the correlation between the hourly values (Table 2), it did not provide a demonstrable solution to the biased shape of the diurnal cycle (Fig. 9). It is possible that the afternoon decline is related to soil moisture effects on stomatal conductance (e.g. Büker et al., 2012), which were not considered here due to lack of data, or to some unidentified factors affecting non-stomatal deposition.

References

- Archibald, A. T., Cooke, M. C., Utembe, S. R., Shallcross, D. E., Derwent, R. G., and Jenkin, M. E.: Impacts of mechanistic changes on HO_x formation and recycling in the oxidation of isoprene, *Atmos. Chem. Phys.*, 10, 8097–8118, 2010.
- Bergström, R., Denier van der Gon, H. A. C., Prévôt, A. S. H., Yttri, K. E., and Simpson, D.: Modelling of organic aerosols over Europe (2002–2007) using a volatility basis set (VBS) framework: application of

different assumptions regarding the formation of secondary organic aerosol, *Atmos. Chem. Phys.*, 12, 8499–8527, 2012.

Büker, P., Morrissey, T., Briolat, A., Falk, R., Simpson, D., Tuovinen, J.-P., Alonso, R., Barth, S., Baumgarten, M., Grulke, N., Karlsson, P. E., King, J., Lagergren, F., Matyssek, R., Nunn, A., Ogaya, R., Peñuelas, J., Rhea, L., Schaub, M., Uddling, J., Werner, W., and Emberson, L. D.: DO₃SE modelling of soil moisture to determine ozone flux to forest trees, *Atmos. Chem. Phys.*, 12, 5537–5562, 2012.

Carslaw, K. S., Lee, L. A., Reddington, C. L., Pringle, K. J., Rap, A., Forster, P. M., Mann, G. W., Spracklen, D. V., Woodhouse, M. T., Regayre, L. A., and Pierce, J. R.: Large contribution of natural aerosols to uncertainty in indirect forcing, *Nature*, 503, 67–71, 2013.

Cieslik, S., Tuovinen, J.-P., Baumgarten, M., Matyssek, R., Brito, P., and Wieser, G.: Gaseous exchange between forests and the atmosphere, *Dev. Environ. Sci.*, 13, 19–36.

CLRTAP: Mapping Critical Levels for Vegetation, Chapter III of Manual on methodologies and criteria for modelling and mapping critical loads and levels and air pollution effects, risks and trends, UNECE Convention on Long-range Transboundary Air Pollution, available at www.icpmapping.org, 2014.

Eugster, W. and Haeni, M.: Nutrients or pollutants? Nitrogen deposition to European forests, *Dev. Environ. Sci.*, 13, 37–56.

Fagerli, H. and Aas, W.: Trends of nitrogen in air and precipitation: Model results and observations at EMEP sites in Europe, 1980–2003, *Environ. Poll.*, 154, 448–461, 2008.

Flechard, C. R., Massad, R.-S., Loubet, B., Personne, E., Simpson, D., Bash, J. O., Cooter, E. J., Nemitz, E., and Sutton, M. A.: Advances in understanding, models and parameterizations of biosphere-atmosphere ammonia exchange, *Biogeosciences*, 10, 5183–5225, 2013.

Foley, K. M., Roselle, S. J., Appel, K. W., Bhave, P. V., Pleim, J. E., Otte, T. L., Mathur, R., Sarwar, G., Young, J. O., Gilliam, R. C., Nolte, C. G., Kelly, J. T., Gilliland, A. B., and Bash, J. O.: Incremental testing of the Community Multiscale Air Quality (CMAQ) modeling system version 4.7, *Geosci. Model Dev.*, 3, 205–226, 2010.

Fowler, D., Pilegaard, K., Sutton, M. A., Ambus, P., Raivonen, M., Duyzer, J., Simpson, D., Fagerli, H., Fuzzi, S., Schjoerring, J. K., Granier, C., Neftel, A., Isaksen, I. S. A., Laj, P., Maione, M., Monks, P. S., Burkhardt, J., Daemmgen, U., Neiryneck, J., Personne, E., Wichink-Kruit, R., Butterbach-Bahl, K., Flechard, C., Tuovinen, J.-P., Coyle, M., Gerosa, G., Loubet, B., Altimir, N., Gruenhage, L., Ammann, C., Cieslik, S., Paoletti, E., Mikkelsen, T. N., Ro-Poulsen, H., Cellier, P., Cape, J. N., Horváth, L., Loreto, F., Niinemets, Ü., Palmer, P. I., Rinne, J., Misztal, P., Nemitz, E., Nilsson, D., Pryor, S., Gallagher, M. W., Vesala, T., Skiba, U., Brüggemann, N., Zechmeister-Boltenstern, S., Williams, J., O'Dowd, C., Facchini, M. C., de Leeuw, G., Flossman, A., Chaumerliac, N., and Erisman, J. W.: Atmospheric composition change: Ecosystems–Atmosphere interactions, *Atmos. Environ.*, 43, 5193–5267, 2009.

Ganzeveld, L., Eerdekens, G., Feig, G., Fischer, H., Harder, H., Königstedt, R., Kubistin, D., Martinez, M., Meixner, F. X., Scheeren, H. A., Sinha, V., Taraborrelli, D., Williams, J., Vilà-Guerau de Arellano, J., and Lelieveld, J.: Surface and boundary layer exchanges of volatile organic compounds, nitrogen oxides and ozone during the GABRIEL campaign, *Atmos. Chem. Phys.*, 8, 6223–6243, 2008.

Gao, W., Wesely, M. L., and Doskey, P. V.: Numerical modeling of the turbulent diffusion and chemistry of NO_x, O₃, isoprene, and other reactive trace gases in and above a forest canopy, *J. Geophys. Res.*, 98, 18339–18353, 1993.

Guenther, A., Hewitt, C. N., Erickson, D., Fall, R., Geron, C., Graedel, T., Harley, P., Klinger, L., Lerdau, M., McKay, W. A., Pierce, T., Scholes, B., Steinbrecher, R., Tallamraju, R., Taylor, J., and Zimmerman, P.: A global model of natural volatile organic compound emissions, *J. Geophys. Res.*, 100, 8873–8892, 1995.

Hertel, O., Christensen, J., Runge, E. H., Asman, W. A. H., Berkowicz, R., and Hovmand, M.: Development and testing of a new variable scale air pollution model – ACDEP, *Atmos. Environ.*, 29, 1267–1290, 1995.

- Hov, Ø.: One-dimensional vertical model for ozone and other gases in the atmospheric boundary layer, *Atmos. Environ.*, 17, 535–549, 1983.
- Jenkin, M. E., Watson, L. A., Utembe, S. R., and Shallcross, D. E.: A Common Representative Intermediates (CRI) mechanism for VOC degradation. Part 1: Gas phase mechanism development, *Atmos. Environ.*, 42, 7185–7195, 2008.
- Jonson, J. E., Stohl, A., Fiore, A. M., Hess, P., Szopa, S., Wild, O., Zeng, G., Dentener, F. J., Lupu, A., Schultz, M. G., Duncan, B. N., Sudo, K., Wind, P., Schulz, M., Marmer, E., Cuvelier, C., Keating, T., Zuber, A., Valdebenito, A., Dorokhov, V., De Backer, H., Davies, J., Chen, G. H., Johnson, B., Tarasick, D. W., Stübi, R., Newchurch, M. J., von der Gathen, P., Steinbrecht, W., and Claude, H.: A multi-model analysis of vertical ozone profiles, *Atmos. Chem. Phys.*, 10, 5759–5783, 2010.
- Kramm, G., Dlugi, G., Dollard, G. J., Foken, T., Mölder, N., Müller, H., Seiler, W., and Sievering, H.: On the dry deposition of ozone and reactive nitrogen species, *Atmos. Environ.*, 29, 3209–3231, 1995.
- Lamarque, J.-F., Shindell, D. T., Josse, B., Young, P. J., Cionni, I., Eyring, V., Bergmann, D., Cameron-Smith, P., Collins, W. J., Doherty, R., Dalsoren, S., Faluvegi, G., Folberth, G., Ghan, S. J., Horowitz, L. W., Lee, Y. H., MacKenzie, I. A., Nagashima, T., Naik, V., Plummer, D., Righi, M., Rumbold, S. T., Schulz, M., Skeie, R. B., Stevenson, D. S., Strode, S., Sudo, K., Szopa, S., Voulgarakis, A., and Zeng, G.: The Atmospheric Chemistry and Climate Model Intercomparison Project (ACCMIP): overview and description of models, simulations and climate diagnostics, *Geosci. Model Dev.*, 6, 179–206, 2013.
- Leuning, R.: Estimation of scalar source/sink distributions in plant canopies using Lagrangian dispersion analysis: Corrections for atmospheric stability and comparison with a multilayer canopy model, *Bound.-Lay. Meteor.*, 96, 293–314, 2000.
- Makar, P. A., Fuentes, J. D., Wang, D., Staebler, R. M., and Wiebe, H. A.: Chemical processing of biogenic hydrocarbons within and above a temperate deciduous forest, *J. Geophys. Res.*, 104, 3581–3603, 1999.
- Meyers, T. P. and Baldocchi, D. D.: A comparison of models for deriving dry deposition fluxes on O₃ and SO₂ to a forest canopy, *Tellus*, 40B, 270–284, 1988.
- Nemitz, E., Sutton, M. A., Wyers, G. P., and Jongejan, P. A. C.: Gas-particle interactions above a Dutch heathland: I. Surface exchange fluxes of NH₃, SO₂, HNO₃ and HCl, *Atmos. Chem. Phys.*, 4, 989–1005, 2004.
- Patankar, S.V.: *Numerical Heat Transfer and Fluid Flow*, Series in Computational Methods in Mechanics and Thermal Sciences, McGraw-Hill, New York, 1980.
- Pleim, J. E., Bash, J. O., Walker, J. T., and Cooter, E. J.: Development and evaluation of an ammonia bidirectional flux parameterization for air quality models, *J. Geophys. Res.*, 118, 3794–3806, 2013.
- Saylor, R. D.: The Atmospheric Chemistry and Canopy Exchange Simulation System (ACCESS): model description and application to a temperate deciduous forest canopy, *Atmos. Chem. Phys.*, 13, 693–715, 2013.
- Schaap, M., Cuvelier, C., Hendriks, C., Bessagnet, B., Baldasano, J. M., Colette, A., Thunis, P., Karam, D., Fagerli, H., Graff, A., Kranenburg, R., Nyiri, A., Pay, M.T., Rouil, L., Schulz, M., Simpson, D., Stern, R., Terrenoire, E., and Wind, P.: Performance of European chemistry transport models as function of resolution, *Atmos. Environ.*, 112, 90–105, 2015.
- Simpson, D.: Biogenic emissions in Europe, 2. Implications for ozone control, *J. Geophys. Res.*, 100, 22891–22906, 1995.
- Simpson, D., Ashmore, M. R., Emberson, L., and Tuovinen, J.-P.: A comparison of two different approaches for mapping potential ozone damage to vegetation. A model study, *Environ. Poll.*, 146, 715–725, 2007.
- Simpson, D., Benedictow, A., Berge, H., Bergström, R., Emberson, L. D., Fagerli, H., Flechard, C. R., Hayman, G. D., Gauss, M., Jonson, J. E., Jenkin, M. E., Nyíri, A., Richter, C., Semeena, V. S., Tsyro, S., Tuovinen, J.-P., Valdebenito, Á., and Wind, P.: The EMEP MSC-W chemical transport model – technical description, *Atmos. Chem. Phys.*, 12, 7825–7865, 2012.

- Simpson, D., Andersson, C., Christensen, J. H., Engardt, M., Geels, C., Nyiri, A., Posch, M., Soares, J., Sofiev, M., Wind, P., and Langner, J.: Impacts of climate and emission changes on nitrogen deposition in Europe: a multi-model study, *Atmos. Chem. Phys.*, 14, 6995–7017, 2014.
- Sutton, M. A., Schjørring, J. K., and Wyers, W. P.: Plant–atmosphere exchange of ammonia, *Phil. Trans R. Soc. Lond. A*, 251, 261–278, 1995.
- Tuovinen, J.-P., Emberson, L., and Simpson, D.: Modelling ozone fluxes to forests for risk assessment: status and prospects, *Ann. For. Sci.*, 66, 401, 2009.
- Verwer, J. and Simpson, D.: Explicit method for stiff ODEs from atmospheric chemistry, *Appl. Numer. Math.*, 18, 413–430, 1995.
- Vieno, M., Dore, A. J., Stevenson, D. S., Doherty, R., Heal, M. R., Reis, S., Hallsworth, S., Tarrason, L., Wind, P., Fowler, D., Simpson, D., and Sutton, M. A.: Modelling surface ozone during the 2003 heat-wave in the UK, *Atmos. Chem. Phys.*, 10, 7963–7978, 2010.
- Wichink Kruit, R. J., Schaap, M., Sauter, F. J., van Zanten, M. C., and van Pul, W. A. J.: Modeling the distribution of ammonia across Europe including bi-directional surface–atmosphere exchange, *Biogeosciences*, 9, 5261–5277, 2012.
- Wolfe, G. M. and Thornton, J. A.: The Chemistry of Atmosphere-Forest Exchange (CAFE) Model – Part 1: Model description and characterization, *Atmos. Chem. Phys.*, 11, 77–101, 2011.
- Yarwood, G., Rao, S., Yocke, M., and Whitten, G.: Updates to the carbon bond chemical mechanism: CB05, Report to US EPA, RT-0400675, available at www.camx.com, 2005.
- Zhang, L., Moran, M. D., and Brook, J. R.: A comparison of models to estimate in-canopy photosynthetically active radiation and their influence on canopy stomatal resistance, *Atmos. Environ.*, 35, 4463–4470, 2001.
- Zhang, L., Wright, L. P., and Asman, W. A. H.: Bi-directional air-surface exchange of atmospheric ammonia: A review of measurements and a development of a big-leaf model for applications in regional-scale air-quality models, *J. Geophys. Res.*, 115, D20310, 2010.

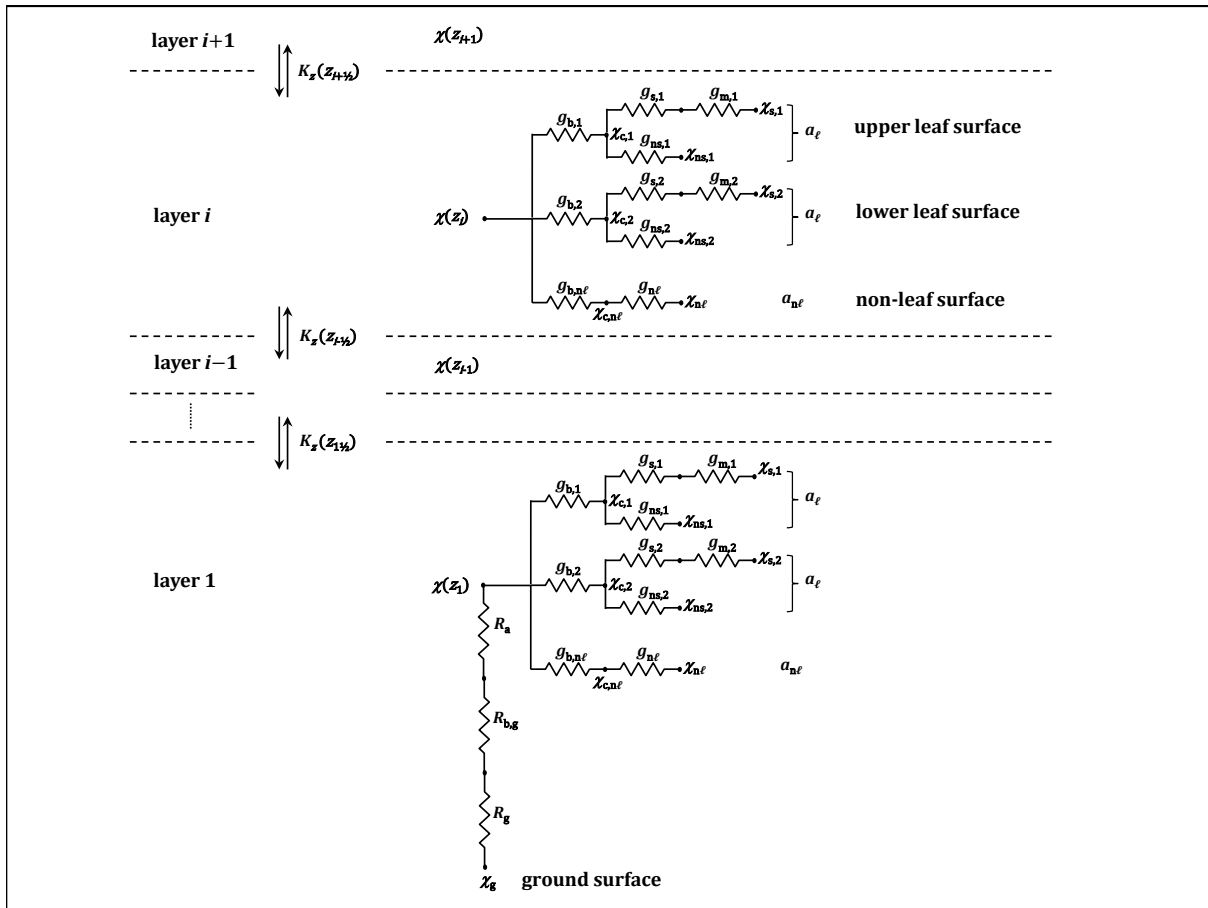


Figure 1. Sketch of the main exchange pathways of the ESX model. Within each layer, bi-directional exchange is calculated separately for upper and lower leaf surfaces ($j = 1, 2$), as well as for non-leaf vegetation and ground surfaces if present. χ = scalar density; $\chi_{c,j}$ = nominal leaf compensation point; $\chi_{c,nl}$ = nominal non-leaf compensation point; $\chi_{s,j}$ = stomatal compensation point; $\chi_{ns,j}$ = non-stomatal leaf compensation point; χ_{nl} = non-leaf surface compensation point; χ_g = soil compensation point; $g_{b,j}$ = leaf boundary layer conductance; $g_{b,nl}$ = non-leaf boundary layer conductance; $g_{s,j}$ = stomatal conductance; $g_{m,j}$ = mesophyll conductance; $g_{ns,j}$ = non-stomatal leaf conductance; g_{nl} = non-leaf surface conductance; R_a = aerodynamic resistance; R_{bg} = soil boundary layer resistance; R_g = soil resistance. The conductances are expressed with respect to surface areas: a_l = projected leaf area distribution; a_{nl} = total non-leaf surface area distribution. The vertical mixing due to turbulence is calculated with eddy diffusivities defined at layer boundaries, $K_z(z_{i+1/2})$. For clarity, the height dependency of the conductance terms and the time dependency of all terms are omitted from the notation.

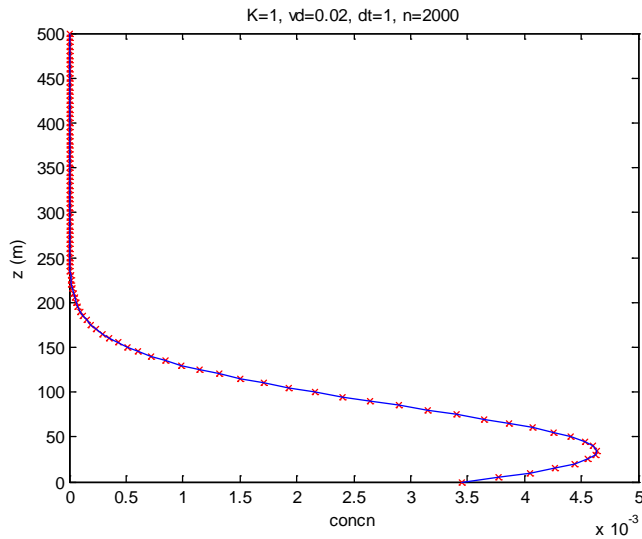


Figure 2. Comparison of numerical (red crosses) and analytical (blue line) solutions of the dispersion-deposition problem: Eqs. (1), (3) and (6) with $S = 0$, $V_d = 0.02 \text{ m s}^{-1}$, $F_0 = 0$, $K_z = 1 \text{ m}^2 \text{ s}^{-1}$. The results show the vertical concentration profile that originates from a continuous ground source after 2000 time steps of 1 s.

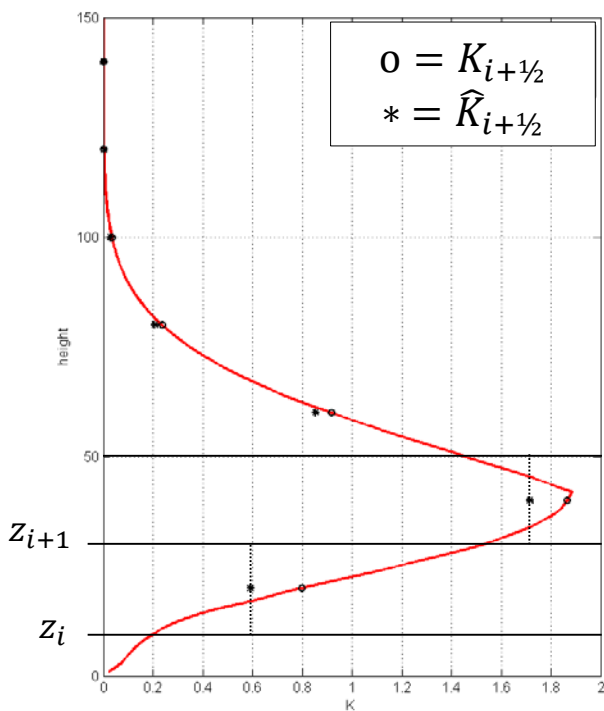


Figure 3. Determination of the effective eddy diffusivity: circles = grid layer values calculated at the layer mid-points; asterisks = effective eddy diffusivity $\hat{K}_{i+1/2} = (z_{i+1} - z_i) / \int_{z_i}^{z_{i+1}} K_z^{-1} dz$.

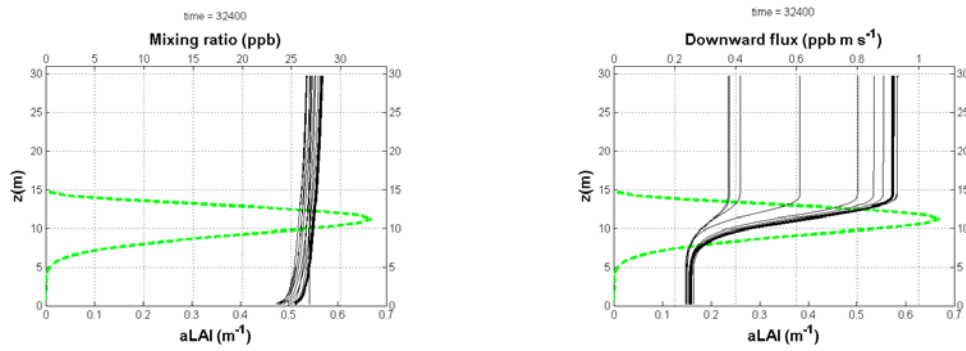


Figure 4. Examples of modelled ozone concentration and flux profiles in the atmospheric surface layer (thick black line = midday; thin lines show the profiles of previous hours). The dashed green line shows the leaf area distribution (aLAI) of a Scots pine forest.

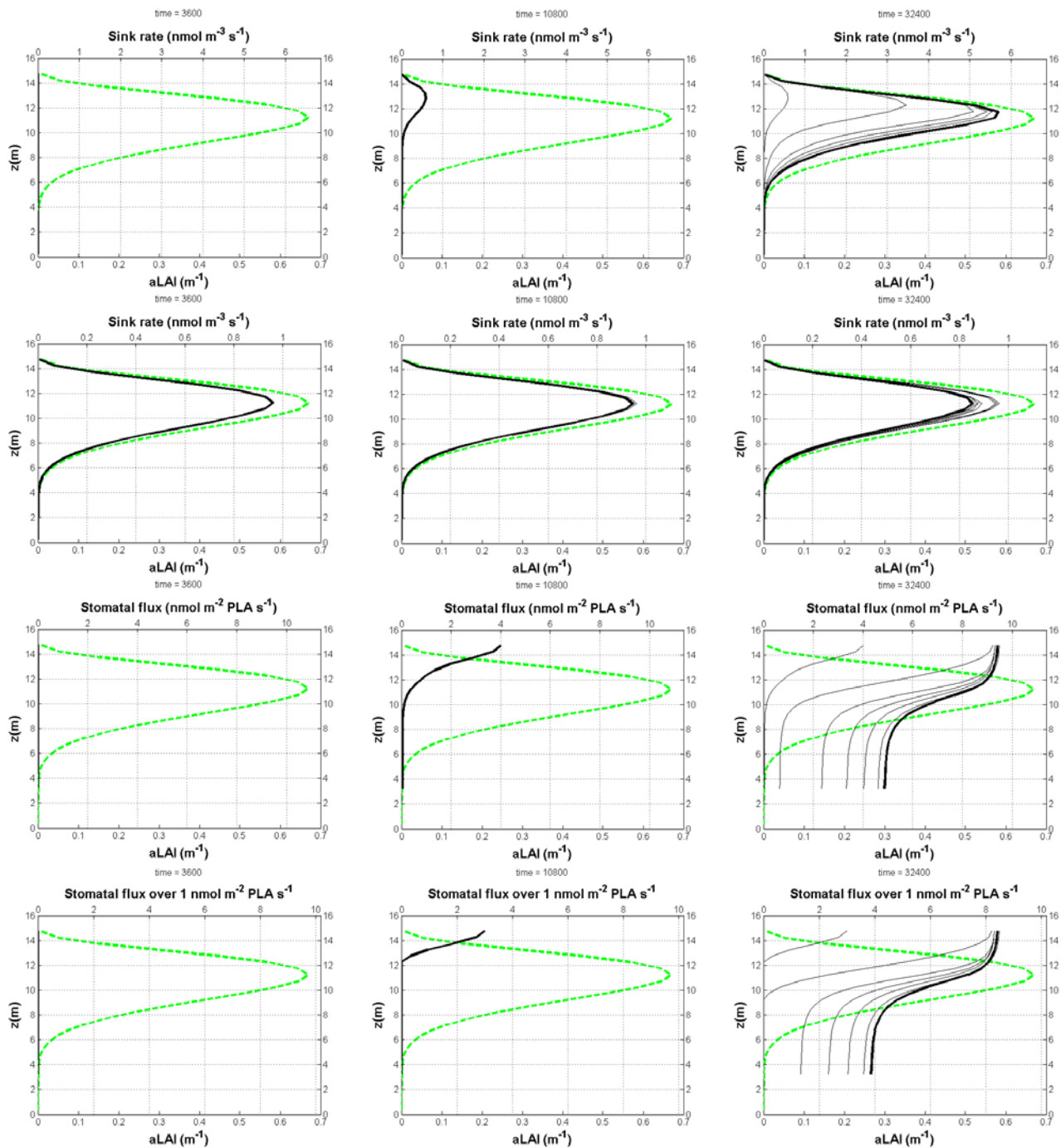


Figure 5. Examples of modelled sink rates and stomatal fluxes of ozone. Rows from top: sink rate due to stomatal deposition, sink rate due to non-stomatal deposition, stomatal flux per leaf area (PLA), stomatal flux over a threshold of $1 \text{ nmol m}^{-2} \text{ s}^{-1}$. Columns from left: night, morning, midday (thick black lines; thin lines show the profiles of previous hours). The dashed green line shows the leaf area distribution (aLAI) of a Scots pine forest.

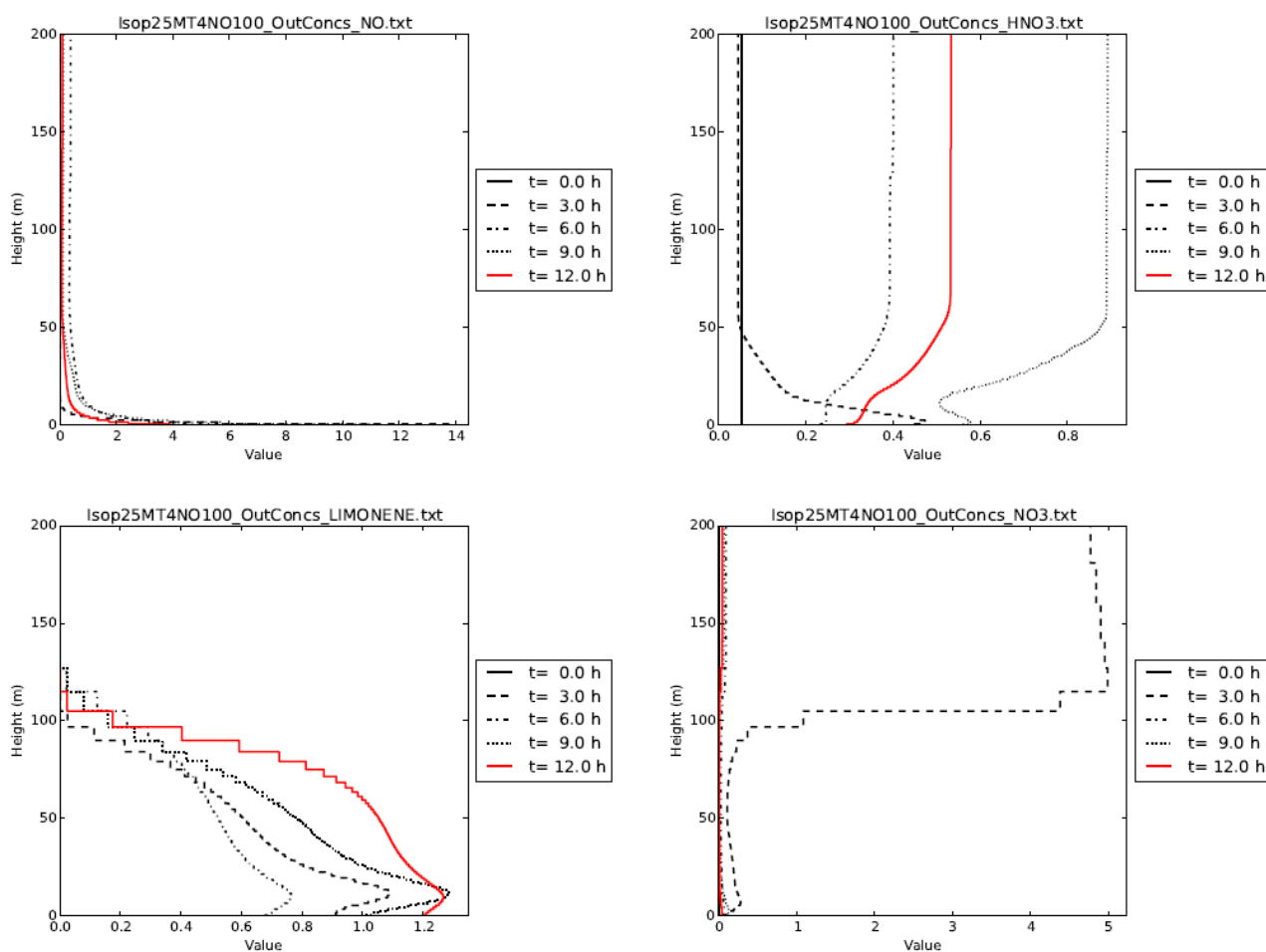


Figure 6. Examples of modelled chemical variability: mixing ratio changes from midnight ($t = 0$) to midday ($t = 12$ h) for a generic deciduous forest with high BVOC and soil-NO emissions. Results are given for NO (top-left), HNO₃ (top-right), limonene (bottom-left) and NO₃ radical (bottom-right). All mixing ratios are in ppb.

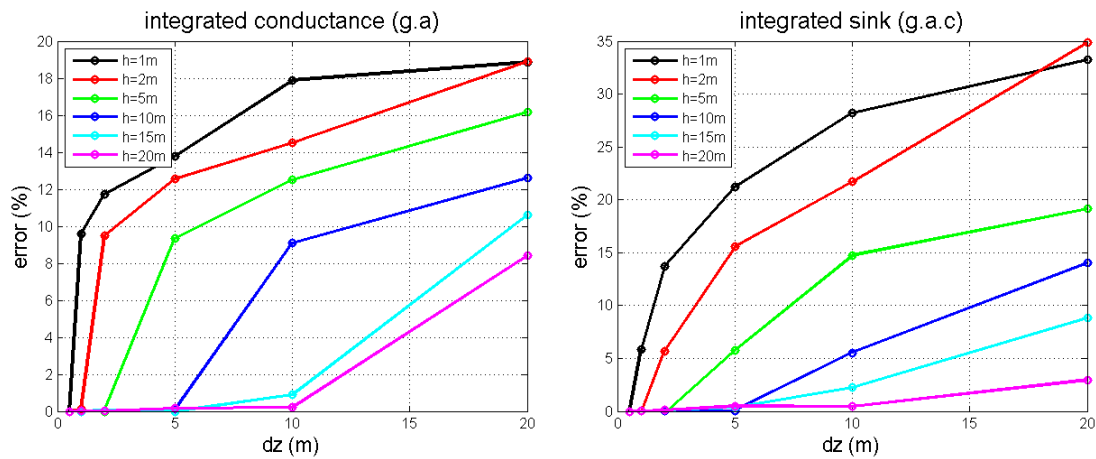


Figure 7. Error in the vertically integrated stomatal conductance $g_{sm}a_\ell$ and sink rate $g_{sm}a_\ell\chi_c$ as a function of grid resolution for different vegetation heights. The calculations are for daytime conditions in midsummer in a Scots pine forest (input derived for Hyytiälä, Finland).

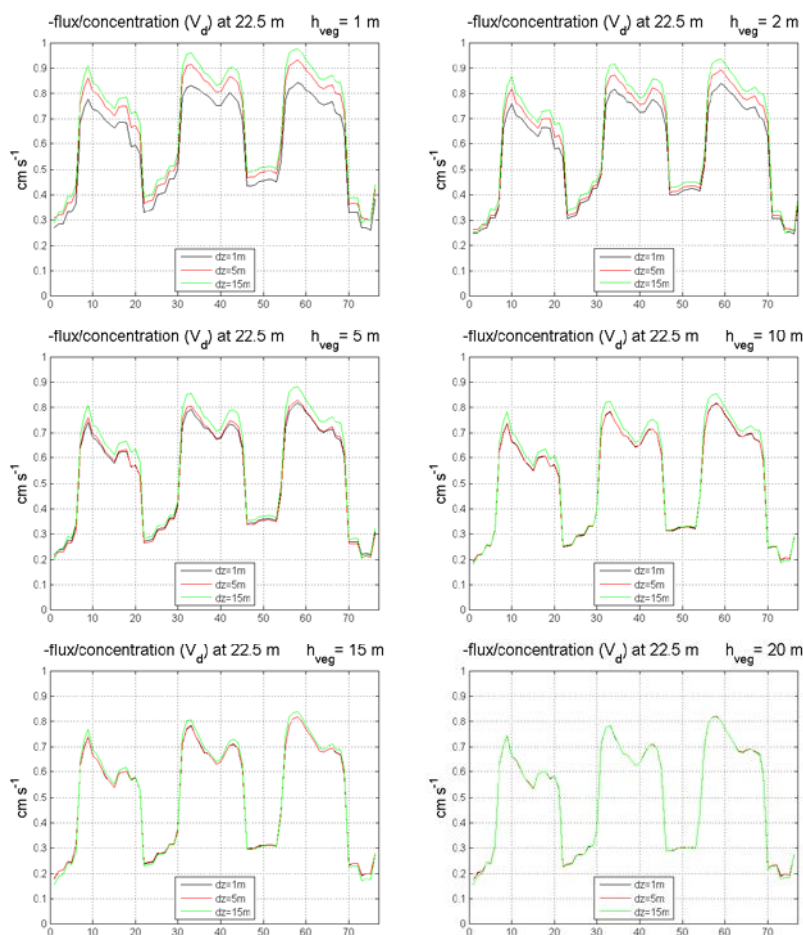


Figure 8. Downward flux/concentration ratio above a Scots pine forest over a 76-h period for different vegetation heights and grid resolutions (input for Hyytiälä, Finland, July 2011).

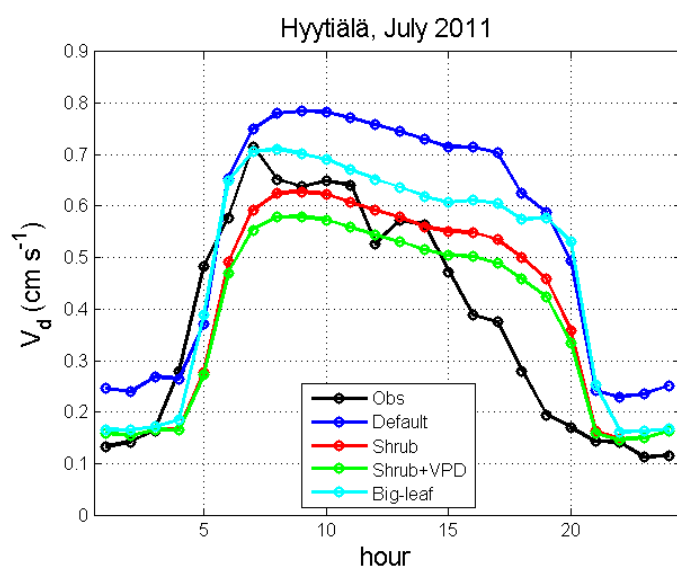


Figure 9. Comparison of the modelled and measured (Obs) ozone deposition velocities at Hyytiälä, Finland. The data show the mean diurnal cycles in July 2011. 'Default' = ESX with parameter values derived from the EMEP/DO₃SE big-leaf model; 'Shrub' = ESX with explicit shrub layer; 'Shrub+VPD' = ESX with explicit shrub layer and more sensitive VPD response; 'Big-leaf' = old EMEP/DO₃SE model.

Annex 2: Simulations with the improved MLM-CHEM system

The ECLAIRE modelling activities focusing on simulation of canopy exchange processes involved two modelling systems; 1) development of a canopy representation in the EMEP modelling system called ESX and 2) further development and application of the Multi-Layer Canopy Chemical Exchange Model (MLC-CHEM) system. MLC-CHEM, which was initially developed and applied in its implementation in a 1-D as well as a global chemistry-climate modelling system (Ganzeveld et al., 2002a and 2002b), is now available as a stand-alone modelling system also to facilitate implementation in other be applied in studies that focus on the analysis of field observations of atmosphere-biosphere exchange processes. As such, the model can be constrained with the observed surface layer micro-meteorology as well as the concentrations of long-lived tracers such as ozone and NO_x to assess the role of in-canopy sources and sinks on calculated in-canopy and mixed layer concentrations and fluxes of reactive compounds. The model, which was in its initial implementation only considering two canopy layers (crown- and understorey layer) has now been extended with a Crank-Nicolson solver that allows to calculate the atmosphere-biosphere exchange using a flexible number of canopy layers. This also allows use of the model in a validation of canopy observations at more than two reference heights inside the canopy. The flexible selection of the number of canopy layers also make it possible to analyse to further assess how resolution affects the simulation of atmosphere-biosphere fluxes where application of MLC-CHEM/ESX in CTMs would preferably require a minimum number of layers for CPU-considerations (Ganzeveld et al., 2002a, showed that two layers suffice to realistically simulate O_3 , NO_x and isoprene canopy top fluxes for tropical forest. However, this might be different for other ecosystems and other compounds, e.g., NH_3 - HNO_3 - NH_4NO_3).

The implementation of MLC-CHEM in the 1-D chemistry-climate model system has been further coupled to the Dynamical Global Vegetation Model (DGVM) LPJGUESS to study the potential relevance of feedbacks involved in the O_3 deposition impact on ecosystem functioning. LPJGUESS has been extended with a first representation of the O_3 deposition impact on NPP and which affects the biogenic emissions of Volatile Organic Compounds (BVOCs) (Arneth et al., 2007), which in turn affect the O_3 production in the boundary layer (BL) and, consequently, O_3 deposition. This coupled system was applied for a study that focussed on the Boreal forest site Hyytiälä, Finland, including an evaluation of the simulated atmosphere-biosphere exchange using field observations in one of the intensive field campaigns conducted at this site, the HUMPPA/COPEC field campaign (Williams et al., 2011). The model study included a first ~100 yr offline simulation with LPJ-GUESS on ecosystem dynamics for this site driven by the CRU climate dataset followed by a fully coupled 1-D chemistry-climate-LPJGUESS simulation for spring/summer 2010 for comparison with field observations. The long-term offline simulations as well as the seasonal online simulation revealed that in assessments of such pollution-biosphere-BL interactions and feedback mechanisms there is an important role of changes in the hydrological cycle. Figure 1 shows for example that under the assumption that there would be a significant O_3 deposition impact on net primary productivity (which is actually not the case for this particular site), changes in the evapotranspiration are minor. This implies also minor changes in BL dynamics and as such in O_3 concentrations and deposition. Another outcome of the extensive evaluation of the seasonal online simulations was that the simulated temporal variability in isoprene and terpene concentrations was very different compared to the observed temporal variability. This indicates that, despite considering state-of the art knowledge on the mechanisms involved in the emissions, transport and chemical processing as function of key meteorological and biogeochemical drivers of this exchange, that there appears to be still a large challenge in reproducing local-scale and short term variability in these reactive compound exchange processes involved in pollution-ecosystem interactions and feedback mechanisms.

MLC-CHEM has also been further developed and applied within ECLAIRE in support of the design of new field campaigns. Figure 2 shows application of MLC-CHEM in a detailed analysis of in-canopy NO_x concentrations as a function of different assumptions on leaf-scale NO_x exchange. Comparison of the observed and simulated in-canopy diurnal cycle in NO_x concentrations for a deciduous forest

site revealed that the best agreement between simulated and observed temporal variability was achieved considering the potential role of a leaf-scale NO_2 compensation point. These results have now been used to also pursue a follow-up measurement activity to study in more detail the role of the compensation point for this specific field site. Such exercises with multi-layer exchange model systems such as MLC-CHEM (and ESX) that can be also applied in CTMs, demonstrate the benefits of model application in terms of 1) supporting field observations that include in-canopy and surface layer atmosphere-biosphere exchange processes and 2) the design of follow-up strategies to improve our understanding and quantification of atmosphere-biosphere exchange processes.

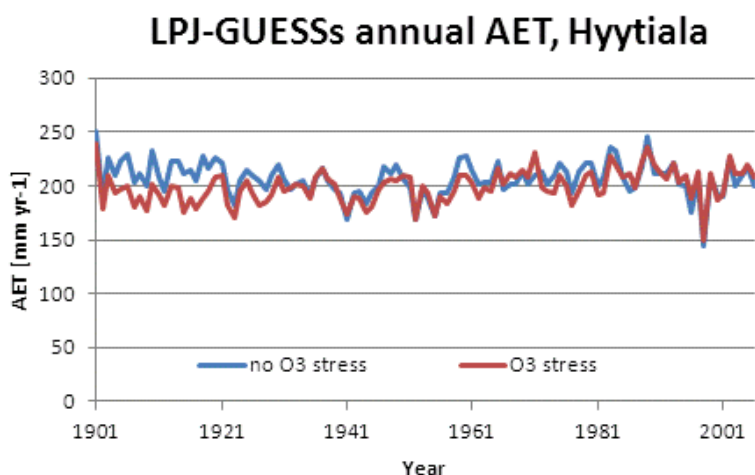


Figure 1: Simulated Annual evapotranspiration rate [mm yr⁻¹] with LPJ-GUESS for Hyttiala, Finland including the potential role of the O_3 deposition impact on NPP.

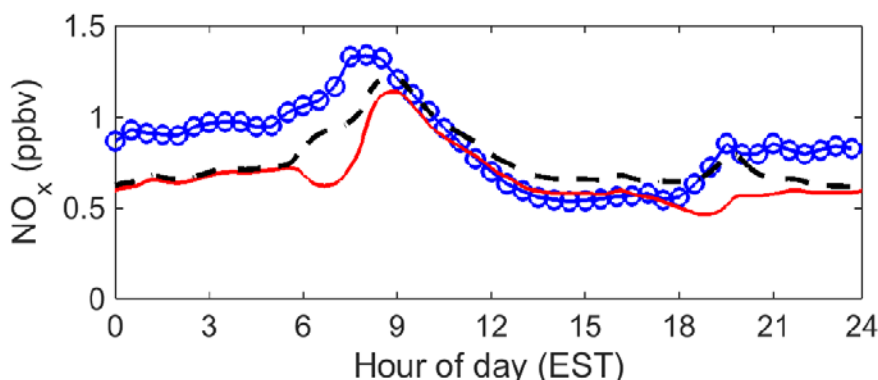


Figure 2: Comparison of the observed and simulated diurnal cycle in NO_x mixing ratios at 15m inside a deciduous forest. The observations are reflected by the blue circles/line. The nocturnal underestimation in the default simulation (red line) is also due to a misrepresentation of soil NO emissions and in-canopy turbulent transport. The black dotted line reflects the simulation that considers the existence of an NO_2 compensation point.

References:

Arneth et al., Process based estimates of terrestrial ecosystem isoprene emissions: Incorporating the effects of a direct CO_2 -isoprene interaction, *Atmos. Chem. Phys.*, 7, 31–53, 2007, <http://www.atmos-chem-phys.net/7/31/2007/>.

Ganzeveld, L., Lelieveld, J., Dentener, F.J., Krol, M.C., Roelofs, G.-J., Atmosphere-biosphere trace gas exchanges simulated with a single-column model, *J. Geophys. Res.* 107, 10.1029/2001JD000684, 2002a.

Ganzeveld, L., Lelieveld, J., Dentener, F.J., Krol, M.C., Bouwman, A.F., and Roelofs, G.-J., The influence of soil-biogenic NO_x emissions on the global distribution of reactive trace gases: the role of canopy processes, *J. Geophys. Res.*, 107, doi: 10.1029/2001JD001289, 2002b.

Williams et al., The summertime Boreal forest field measurement intensive (HUMPPA-COPEC-2010): an overview of meteorological and chemical influences, *Atmos. Chem. Phys.*, 11, 10599–10618, 2011